PROOF COVER SHEET

Author(s):	Reza Beheshti
Article Title:	Reduction kinetics of commercial haematite pellet in a fixed bed at 1123–1273 K
Article No:	YIRS1104072
Enclosures:	1) Query sheet
	2) Article proofs

Dear Author,

1. Please check these proofs carefully. It is the responsibility of the corresponding author to check these and approve or amend them. A second proof is not normally provided. Taylor & Francis cannot be held responsible for uncorrected errors, even if introduced during the production process. Once your corrections have been added to the article, it will be considered ready for publication.

Please limit changes at this stage to the correction of errors. You should not make trivial changes, improve prose style, add new material, or delete existing material at this stage. You may be charged if your corrections are excessive (we would not expect corrections to exceed 30 changes).

For detailed guidance on how to check your proofs, please paste this address into a new browser window: http://journalauthors.tandf.co.uk/production/checkingproofs.asp

Your PDF proof file has been enabled so that you can comment on the proof directly using Adobe Acrobat. If you wish to do this, please save the file to your hard disk first. For further information on marking corrections using Acrobat, please paste this address into a new browser window: http://journalauthors.tandf.co.uk/production/acrobat.asp

2. Please review the table of contributors below and confirm that the first and last names are structured correctly and that the authors are listed in the correct order of contribution. This check is to ensure that your name will appear correctly online and when the article is indexed.

Sequence	Prefix	Given name(s)	Surname	Suffix
1		Reza	Beheshti	
2		John	Moosberg-Bustnes	
3		Mark W.	Kennedy	
4		Ragnhild E.	Aune	

Queries are marked in the margins of the proofs, and you can also click the hyperlinks below.

AUTHOR QUERIES

General points:

1. **Permissions**: You have warranted that you have secured the necessary written permission from the appropriate copyright owner for the reproduction of any text, illustration, or other material in your article. Please see http://journalauthors.tandf.co.uk/permissions/usingThirdPartyMaterial.asp.
2. **Third-party content**: If there is third-party content in your article, please check that the rightsholder details for re-use are shown correctly.
3. **Affiliation**: The corresponding author is responsible for ensuring that address and email details are correct for all the co-authors. Affiliations given in the article should be the affiliation at the time the research was conducted. Please see http://journalauthors.tandf.co.uk/preparation/writing.asp.
4. **Funding**: Was your research for this article funded by a funding agency? If so, please insert 'This work was supported by <insert the name of the funding agency in full>', followed by the grant number in square brackets '[grant number xxxx]'.
5. **Supplemental data and underlying research materials**: Do you wish to include the location of the underlying research materials (e.g. data, samples or models) for your article? If so, please insert this sentence before the reference section: 'The underlying research materials for this article can be accessed at <full link>/ description of location [author to complete]'. If your article includes supplemental data, the link will also be provided in this paragraph. See <http://journalauthors.tandf.co.uk/preparation/multimedia.asp> for further explanation of supplemental data and underlying research materials.

QUERY NO.	QUERY DETAILS
AQ1	Please check whether the inserted running head is Ok?
AQ2	Please note that the journal requires a minimum of five to seven keywords. Please insert additional keywords accordingly.
AQ3	The CrossRef database (www.crossref.org/) has been used to validate the references. Mismatches between the original manuscript and CrossRef are tracked in red font. Please provide a revision if the change is incorrect. Do not comment on correct changes
AQ4	Please provide the page range for reference [16]
AQ5	Please provide the volume number and page range for reference [25]
AQ6	Please provide the volume number and page range for reference [33]

How to make corrections to your proofs using Adobe Acrobat/Reader

Taylor & Francis offers you a choice of options to help you make corrections to your proofs. Your PDF proof file has been enabled so that you can edit the proof directly using Adobe Acrobat/Reader. This is the simplest and best way for you to ensure that your corrections will be incorporated. If you wish to do this, please follow these instructions:

1. Save the file to your hard disk.

2. Check which version of Adobe Acrobat/Reader you have on your computer. You can do this by clicking on the "Help" tab, and then "About".

If Adobe Reader is not installed, you can get the latest version free from http://get.adobe.com/reader/.

3. If you have Adobe Acrobat/Reader 10 or a later version, click on the "Comment" link at the right-hand side to view the Comments pane.

4. You can then select any text and mark it up for deletion or replacement, or insert new text as needed. Please note that these will clearly be displayed in the Comments pane and secondary annotation is not needed to draw attention to your corrections. If you need to include new sections of text, it is also possible to add a comment to the proofs. To do this, use the Sticky Note tool in the task bar. Please also see our FAQs here: http://journalauthors.tandf.co.uk/production/index.asp.

5. Make sure that you save the file when you close the document before uploading it to CATS using the "Upload File" button on the online correction form. If you have more than one file, please zip them together and then upload the zip file.

If you prefer, you can make your corrections using the CATS online correction form.

Troubleshooting

Acrobat help: http://helpx.adobe.com/acrobat.html
Reader help: http://helpx.adobe.com/reader.html

Please note that full user guides for earlier versions of these programs are available from the Adobe Help pages by clicking on the link "Previous versions" under the "Help and tutorials" heading from the relevant link above. Commenting functionality is available from Adobe Reader 8.0 onwards and from Adobe Acrobat 7.0 onwards.

Firefox users: Firefox's inbuilt PDF Viewer is set to the default; please see the following for instructions on how to use this and download the PDF to your hard drive: http://support.mozilla.org/en-US/kb/view-pdf-files-firefox-without-downloading-them#w_using-a-pdf-reader-plugin

Reduction kinetics of commercial haematite pellet in a fixed bed at 1123–1273 K

Reza Beheshti*[1,2], John Moosberg-Bustnes[1], Mark W. Kennedy[3,4] and Ragnhild E. Aune[3]

In the present study a model for future use in the modelling of moving bed Direct Reduction reactors has been developed. The model of a fixed bed reactor for the production of sponge iron from haematite incorporates both heat- and mass-transfer, as well as the chemical reduction rate. The model results were compared to the experimental data obtained from a lab scale reactor in the temperature range 1123–1273 K, as well as to the output from a simple model assuming isothermal conditions. The H_2/CO ratio (β) of the reducing gas was in all cases varied from 0.8 to 2.0. Overall the non-isothermal model has been developed permits a more accurate representation of the experimental data than the isothermal estimates, with a typical discrepancy of only 1.3%.

Keywords: Fixed bed, Shrinking Core Model, Gas-solid reaction, Heat transfer

Introduction

Steel is one of the pillars of modern society and it will continue to play this role long into the twenty-first century.[1,2] At present the most common method of converting iron ore to metallic iron utilizes a Blast Furnace (BF) where the material is melted to form hot metal, which in turn is converted to steel in a Basic Oxygen Furnace (BOF). The energy costs are, however, relatively high in the BF-BOF process. The pollution problems associated with ancillary equipment can also be quite severe, and the capital investment requirements are significant.[3–5] As a result the Electric Arc Furnace (EAF) route has been commercialised, and its use is expected to further increase.

The EAF route was initially developed for remelting and recycling of steel scrap. Problems related to the scrap feed, i.e.: (i) short supply, (ii) the heterogeneous nature, (iii) price volatility and above all else (iv) the higher content of tramp elements (Cu, Sn, Cr, Mo, Ni, etc.), necessitated a search for alternative feed materials. This problem is today tackled by using Direct Reduced Iron (DRI) or sponge iron. DRI is not only a substitute for steel scrap as a feed material in EAFs, but also a more suitable melting stock for the production of higher quality steels.[3,4,6–10]

Seventy-five percent of the world's DRI is today produced using one of the two main gas-based processes available, i.e. Midrex and HYL. About 23% of the DRI produced globally is from the coal-based Direct Reduction (DR) processes mainly found in India and South Africa (SL/RN, FASTMET). There are also some other processes, which are not yet considered fully commercialised, e.g. FINMET, CIRCORED.[8,10–14] It is believed that the DR processes will play an increasingly major role in ironmaking in the twenty-first century.[3,4,12] The DR-EAF route produces today 0.8–1.2 t of CO_2 t^{-1} of liquid steel, compared to the BF-BOF route which produces 2–2.25 t CO_2 t^{-1} liquid steel.[12,15]

A review of the literature has revealed a lack of information in regards to the reaction kinetics of the DR processes, especially for the reduction in a fixed bed.[16,17] It is well known that DR reactors are complicated systems due to: (i) multiple reactions proceeding subsequently and/or in parallel, (ii) the diversity in mechanisms of gas–solid reactions and (iii) simultaneous heat- and mass-transfer. In the case of sequential reactions, each intermediate solid is produced from a solid and a gaseous reactant and then subsequently consumed through a further reaction, e.g. $Fe_2O_3 \rightarrow Fe_3O_4 \rightarrow FeO \rightarrow Fe$. In the case of parallel reactions, the same solid may react simultaneously with different gas species (H_2, CO) to produce the same solid product. These different steps in the sequential reduction of iron oxide are either endothermic or mildly exothermic. The reactions do, however, proceed so rapidly[16,18] that isothermal conditions cannot be assured in the whole bed; hence, pellets can deviate in temperature either positively or negatively from the overall average bed temperature. The dynamic variation of temperature, which influences the degree of conversion, makes it necessary to evaluate and take the temperature variation in the bed into consideration. The present authors have chosen to start out with modelling the reduction rate of a single pellet, and to continue with the modelling of a fixed bed with many pellets (~200 pellets). The overall objective is to extend the work to even include an industrial moving-bed reactor.

[1]Northern Research Institute Narvik (Norut Narvik), Narvik NO-8504, Norway
[2]Deparment of Materials Science and Engineering, Royal Institute of Technology (KTH), Stockholm SE-10044, Sweden
[3]Deparment of Materials Science and Engineering, Norwegian University of Science and Technology (NTNU), Trondheim NO-7491, Norway
[4]Proval Partners S.A., Avenue de Sévelin 6b, Lausanne CH-1007, Switzerland

*Corresponding author, email: rezakb@kth.se

Published by Maney on behalf of the Institute
Received 15 July 2015; accepted 21 September 2015
DOI 10.1080/03019233.2015.1104072

As the first step, a model for the reduction rate of a single pellet was developed, and has been reported elsewhere.[19] This isothermal model was based on the Shrinking Core Model (SCM)[20–24] for gas–solid reactions. The model considered the diffusion in the porous haematite pellet, as well as in the product layers, and the equations were solved by Finite Element Modelling (FEM) using the commercial COMSOL Multiphysics® software (Version 4.3b). The model was validated against the results from isothermal single haematite pellet experiments.

The same type of experiments as for a single pellet was also carried out for a 0.5 kg fixed bed in order to determine the impact that the scale up had on the overall rate of reduction. This improved model simulated the reduction rate by considering the composition gradient in the bulk gas, as well as how the concentration gradient changes with the progression of the reduction reaction. The model proved to reproduce the experimental results with a 2.5% deviation.[25] There was, however, a desire to improve the model accuracy further, while at the same time keeping the level of complexity low and the convergence time short.

It is important to point out that during the experiments on a fixed bed, it was established that the reaction rate was relatively high, i.e. approximately 70% reduction was achieved in the first 10 minutes.[25] It is believed that the heat transfer in the porous bed in this case led to variations in local temperatures in spite of the small reactor size. Hence, assuming a constant temperature over the whole bed introduces observable errors into the model.[16] Based on this, the present study revisits and extends the previous developed model to include the effect of the temperature variation and the heat transfer in a fixed bed. Since the prior model was developed by considering both the Reaction and the Mass-transfer rates it will in the present study be referred to as Reaction, Mass transfer Model (RMM), and the model to be developed in the present study considering also the Heat transfer will be referred to as Reaction, Mass transfer, Heat transfer Model (RMHM).

Modelling concept and key assumptions

In the fixed bed, the three dimensional structure that is created by porous pellets makes the modelling of mass- and heat transfer a challenging task. The challenge lies in the description of the macro- and micro-porous structure, which results in an order of magnitude difference between heat- and mass-transfer properties within the pellet compared to between pellets. The most important assumptions often made during modelling of such a reduction process include[17,24–28]:

- The pellets are spherical with a constant diameter and with uniform porosity, as well as without crack formation.
- No temperature gradient exists inside the pellets, and both the gas within the pellet's pores and the solid species are at a constant temperature.
- The pellets in the bed and the gas that surrounds them are on the same temperature.
- The first order reduction reactions are irreversible and controlled by combined chemical reaction and gaseous diffusion.
- The catalytic effects are negligible.
- The bulk gas flow in the reactor is uniform 'plug' flow, i.e. without axial or back-mixing.
- The reactor wall and the gas in contact with the reactor wall are at the same temperature.
- The bed porosity is constant over time.
- The pressure inside the reactor is constant at atmospheric pressure.
- The temperature gradient in the axial direction is negligible.

The above assumptions are also the bases of the present study. As in the previous study the SCM was applied for the modelling of the reaction rates within a single pellet. A series of heterogeneous chemical reactions were considered to take place at the interface of the pellets as they move spatially and change with time over the course of the iron reduction sequence. Even the generation or consumption of heat by the various sequential reactions, as well as heat exchange to the gases surrounding the pellets, were considered; hence, the new model aims to solve the reaction, heat- and mass transport equations simultaneously.

Mass balance

The diffusion equation for each gaseous species may be written as follows:

$$u\nabla C_i + \frac{\partial C_i}{\partial t} + \nabla(D_{\text{eff},i}\nabla C_i) = R_i \quad i = \text{H}_2,\ \text{CO} \tag{1}$$

$$R_{\text{overall}} = \frac{\partial f}{\partial t} = \sum_i \frac{R_i}{(1-\varepsilon_b)} \tag{2}$$

The model for mass-transfer is explained by the present authors in detail elsewhere[19,25].

Heat balance

The energy balance of interest in the system is related to the heat transferred between gas and solid, and the net heat of the sequential reactions, see Table 1. In principle, the energy equation for heat transfer in a porous media should include conduction, radiation and convection; however, the common approach is to simplify the radiant heat transfer at higher temperatures by including it in an effective thermal conductivity term.[26,27,29] In the present study, the enthalpy of reactions were calculated using the FactSage™ software.[30]

The radial thermal dispersion, i.e. wall to centre, is expressed by the following equations[27,31]:

$$\rho C_p \frac{\partial T_b}{\partial t} + \rho C_p u \nabla T_b = \nabla(k_{\text{eff}}\nabla T_b) + \sum_{i=1}^{6}(-\Delta H_i)R + Q \tag{9}$$

$$\frac{\partial Q}{\partial t} = K_{\text{eff}} A_b \frac{\partial T_b}{\partial x} \tag{10}$$

The initial and boundary conditions adapted for equation (9) were:

$$T_b = T_0 \quad \text{at } t >= 0 \text{ (retort wall)}$$
$$\frac{\partial T_b}{\partial z} = 0 \quad \text{at } t >= 0$$

Table 1 The enthalpy of reactions 3–8 calculated at 1123, 1173, 1223 and 1273 K according to Factsage™

Reduction reaction	ΔH°(J/mol)	ΔH°_{T} (kJ mol^{-1})	Equation
$3Fe_2O_3 + H_2 = 2Fe_3O_4 + H_2O$	$0.0493T^2 - 122.32T + 69\,452$	$\Delta H°_{1123} = -5.74$ $\Delta H^{\circ}_{1173} = -6.20$ $\Delta H^{\circ}_{1223} = -6.41$ $\Delta H^{\circ}_{1273} = -6.37$	(3)
$3Fe_2O_3 + CO = 2Fe_3O_4 + CO_2$	$0.037T^2 - 83.525T + 7829.7$	$\Delta H^{\circ}_{1123} = -39.31$ $\Delta H^{\circ}_{1173} = -39.24$ $\Delta H^{\circ}_{1223} = -38.98$ $\Delta H^{\circ}_{1273} = -38.54$	(4)
$Fe_3O_4 + H_2 = 3FeO + H_2O$	$0.0261T^2 - 71.987T + 97\,671$	$\Delta H^{\circ}_{1123} = 49.75$ $\Delta H^{\circ}_{1173} = 49.14$ $\Delta H^{\circ}_{1223} = 48.67$ $\Delta H^{\circ}_{1273} = 48.33$	(5)
$Fe_3O_4 + CO = 3FeO + CO_2$	$0.0228T^2 - 54.682T + 48\,861$	$\Delta H^{\circ}_{1123} = 16.21$ $\Delta H^{\circ}_{1173} = 16.09$ $\Delta H^{\circ}_{1223} = 16.09$ $\Delta H^{\circ}_{1273} = 16.20$	(6)
$FeO + H_2 = Fe + H_2O$	$-13.813T + 33\,219$	$\Delta H^{\circ}_{1123} = 17.71$ $\Delta H^{\circ}_{1173} = 17.02$ $\Delta H^{\circ}_{1223} = 16.33$ $\Delta H^{\circ}_{1273} = 15.64$	(7)
$FeO + CO = Fe + CO_2$	$-5.1505T - 9941.1$	$\Delta H°_{1123} = -15.73$ $\Delta H°_{1173} = -15.98$ $\Delta H°_{1223} = -16.24$ $\Delta H°_{1273} = -16.50$	(8)

Table 2 General literature data for a single pellet and a fixed bed[16]

Apparent density of a single pellet (ρ, kgm^{-3})	Heat capacity of a single pellet (Cp, J kg^{-1} K^{-1})	Effective thermal conductivity of a single pellet (K_{eff}, W m^{-1} K^{-1})	Fixed bed porosity (ε_b)
4222	975.6	0.5	0.5

All general literature data adapted in the present model, for both the individual pellets and the fixed bed, are summarised in Table 2.[16]

Materials and experimental procedure

All the DR pellets used in the present study were of commercial grade, i.e. KPRS pellets supplied by LKAB, Kiruna, Sweden. The chemical composition of the KPRS pellets is summarised in Table 3. The reducing gas atmosphere used during the reduction experiments consisted of a mixture of H_2 and CO, while N_2 was used as an inert gas to prevent unwanted reactions from taking place during the heating and/or cooling cycles.

The experimental set-up used was based on a thermal gravimetric analysis principal as shown in Fig. 1. A schematic view of the set-up, as well as the gas flow in to the retort are given in Fig. 2.[33]

Experiments were conducted using a fixed mass of iron ore pellets (0.5 kg), at four different temperatures, i.e. 1123, 1173, 1223 and 1273 K, and four different reducing gas compositions, i.e. at: $\beta = 0.8$, 1.2, 1.6 and 2. Two additional experiments were carried out using (i) pure H_2 and (ii) pure CO, as a reference case. To keep the flow rate constant, pure reducing gas (H_2 or CO) diluted by approximately 25% vol. N_2 to avoid very high concentrations of flammable gases in the off gas system. A summary of the experimental condition adopted during the present study is given in Table 4 and Table 5.

Table 3 Chemical composition of the KPRS pellets supplied by LKAB, Kiruna, Sweden, in wt-%[32]

Fe	SiO_2	CaO	MgO	Al_2O_3	Mn	P	S
67.9	0.75	0.9	0.65	0.16	0.06	0.025	<0.002

Experimental results and discussion

The temperature measurement at the centre of the bed showed a significant temperature drop during first 10

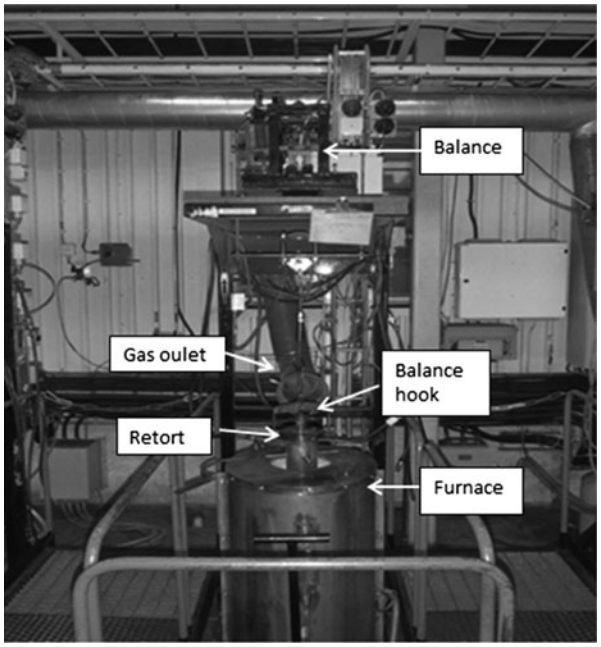

1 A picture of the experimental set-up[25]

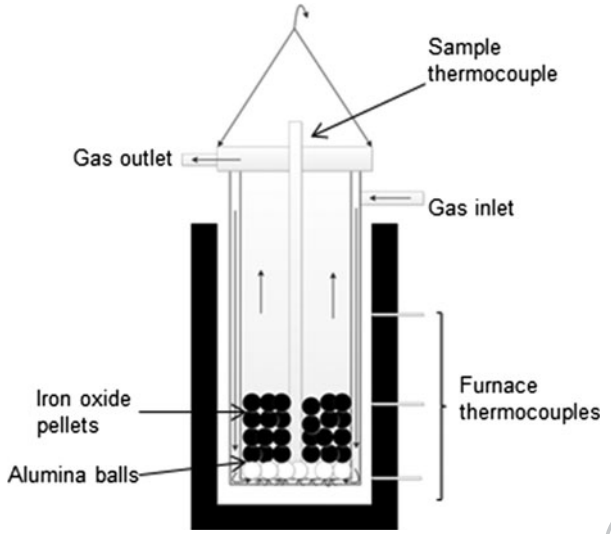

2 A schematic view of the experimental set-up[25]

minutes, as shown in Fig. 3. This phenomenon may be explained by the endothermic nature of the magnetite to wustite reduction reaction, see equations (5) and (6). Initially the reduction reactions are believed to be dominated by H_2,[34–36] but this domination reduces with time as the CO starts to diffuse into the pellet and as the rate of the more exothermic reduction reaction increases, see equation (10). This is supported by the fact that the magnitude of the temperature drop in Fig. 3 proved to be larger for higher contents of H_2 in the reducing gas mixture.

In Fig. 4 the reduction fraction of the fixed bed as a function of time at 1173 K with changing gas compositions (β), from pure H_2 ($\beta = \infty$) to pure CO ($\beta = 0$), is presented. From the figure it can be seen that with an increasing H_2 concentration in the reducing gas mixture, the reduction rate increases.

Based on the obtained results it was established that the initial reaction rate during the first 2 minutes increased from 6% min^{-1} to 11% min^{-1} with the use of H_2. It can furthermore be seen that all of the gas mixtures containing H_2 reacted at a similar initial rate, substantially validating the conclusion that initially H_2 is the dominant reducing species. It is only after 10 minutes that the reduction reactions containing CO appear to become significant.

In the case of the experiments conducted in pure CO the reduction did not reach completion within the duration of the experiments, i.e. 60 minutes. As can be seen from Fig. 4, only 88% reduction was reached and the reaction product proved to be wustite.[37–39] On the other hand, the reduction by pure H_2 reached 99% completion within the first 25 minutes. It can therefore be concluded that the conditions were favourable for fast reduction by H_2. It should be pointed out that the endothermic H_2 reactions did not experience any limitation due to sensible heat as the gas temperature and the flow rate were both high. It

Table 5 The temperature and gas compositions used in each of the experiments

H_2/CO (β)	1:0	0.8:1	1.2:1	1.6:1	2:1	0:1
T(K)						
1123		*		*		
1173	*	*	*	*	*	*
1223		*	*	*	*	
1273		*		*		

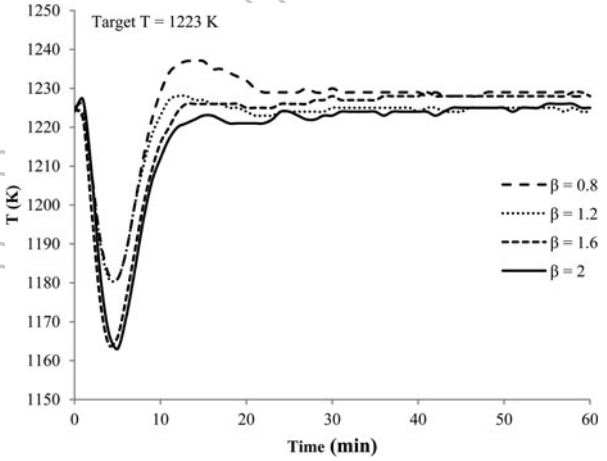

3 The temperature of the fixed bed as a function of time during the reduction process for various β, i.e. H_2/CO, and at a set temperature of 1223 K

can also be seen from Fig. 4 that in the case of the experiments conducted with a gas mixture of H_2/CO, the samples were fully reduced within 30 min.

In Fig. 5 the reduction fraction of the fixed bed as a function of time at 1223 K with changing gas compositions is presented. As can be seen from the figure, the effect of the gas composition gets weaker with time, i.e. the total degree of reduction converges after 20–25 minutes. Furthermore, the rate of reaction by $\beta = 1.2$ and 1.6 overlap throughout the reduction period and the difference in the reduction rates is not distinguishable. At 1173 K a similar convergence after long reduction time (about 30 minutes) can be seen at $\beta = 1.6$ and $\beta = 2$. Therefore, the relative contribution of the higher reaction rate of H_2 to the overall rate appears to be reduced at higher temperatures and longer reaction times.

In Fig. 6 the comparison of the change of the reduction fraction versus time at two different gas ratios, i.e. 0.8 and 1.6, for a number of different temperatures, i.e. 1123, 1173, 1123 and 1273 K, is presented. As can be seen from the figure the reduction fraction for any given time at each of these gas compositions shows that an increase in temperature allows for an increase in the total degree reduced. The effect is more pronounced when the reducing gas mixture was rich in H_2, which may well be

Table 4 Overall experimental conditions

Holding time (min)	Sample weight (kg)	Gas flow (Nl min^{-1})	Pellets size (mm)	Oxygen content of the pellets (%)	Porosity of the pellet (%)	Bed depth (mm)
60	0.5	50	10–12.5	29.1	27	60

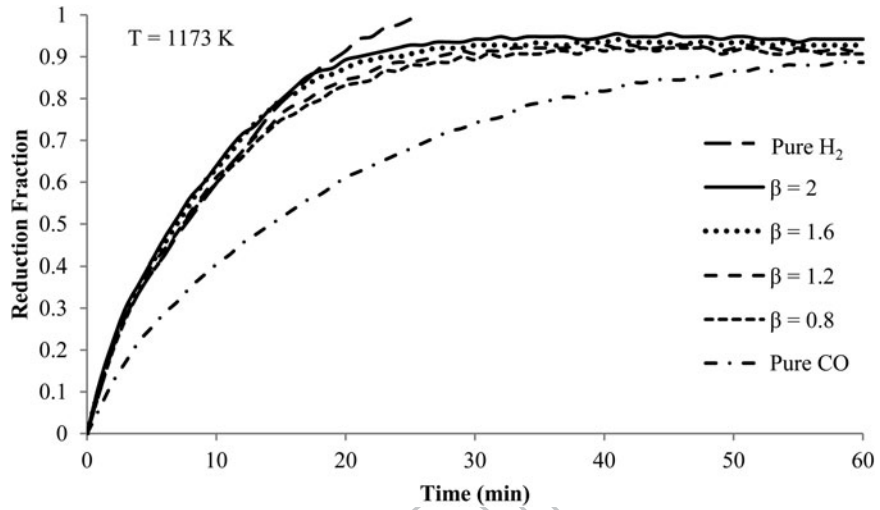

4 The reduction fraction of the fixed bed as a function of time at 1173 K for various β, i.e. H_2/CO

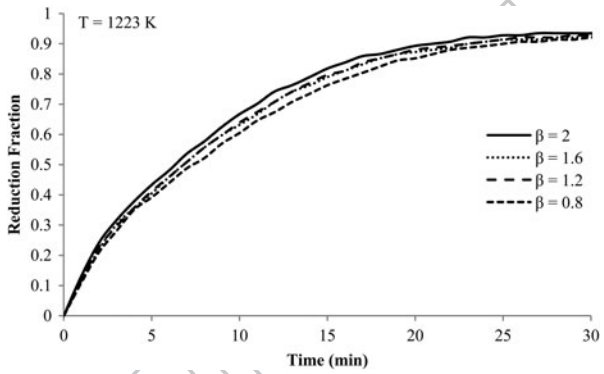

5 The reduction fraction of the fixed bed as a function of time at 1223 K for various β, i.e. H_2/CO

supported by the endothermic reaction by H_2. Moreover, except for two outliers, i.e. $\beta = 0.8$ at 1123 K and $\beta = 1.6$ at 1273 K, all of the experiments reached 0.92 reduction fraction within 30 minutes. The obtained results show that potential exists for optimisation between the temperature and gas ratio (β), based on both economic and technical requirements.

Modelling results and discussion

In this section the experimental results presented in the previous section are compared against predictions of the RMHM developed in the present study. The accuracy of the RMHM is compared against predictions using the RMM (previously developed)[25] under similar conditions. In order to quantitatively calculate the accuracy of the model, an error analysis is performed using following relationship[40]:

$$e = \left(\frac{1}{N} \sum_{i=1}^{N} \frac{(f_{\exp,i} - f_{\mathrm{mod},i})^2}{f_{\exp,i} f_{\mathrm{mod},i}} \right) 100\% \qquad (11)$$

In Table 6 the accuracy of the RMM and the RMHM, calculated at 1173 K, is presented. As can be seen from table, the division between the experimental results and the RMHM results gives a constant error of 1.1% for all four gas mixtures. In the case of the RMM the division

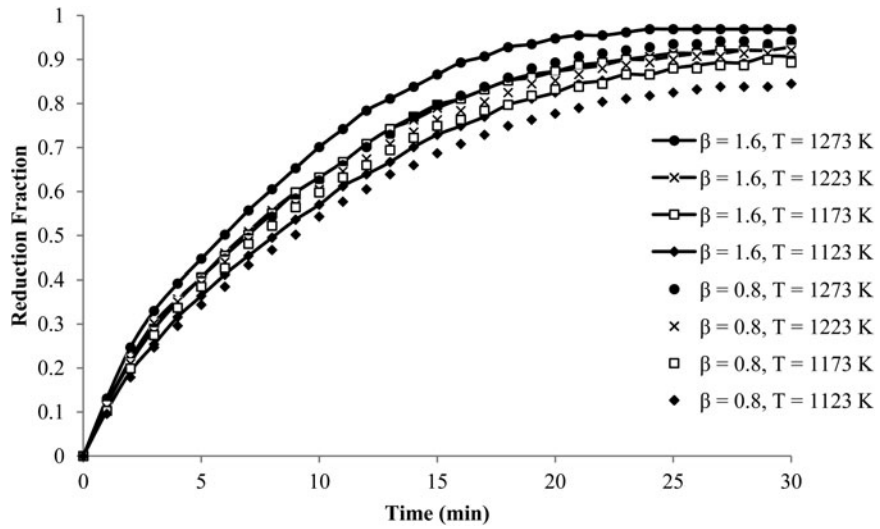

6 The reduction fraction of the fixed bed as a function of time in the temperature interval 1123–1273 K for various β, i.e. H_2/CO; (i) $\beta = 0.8$ and (ii) $\beta = 1.6$

Table 6 The accuracy of the RMM and the RMHM, calculated at 1173 K using equation (13), for various ratios of H_2/CO, i.e. (β)

β	0.8	1.2	1.6	2	Average
Model error					
RMM	2.1	2.2	2.6	3	2.5
RMHM	1.1	1.1	1.1	1.1	1.1

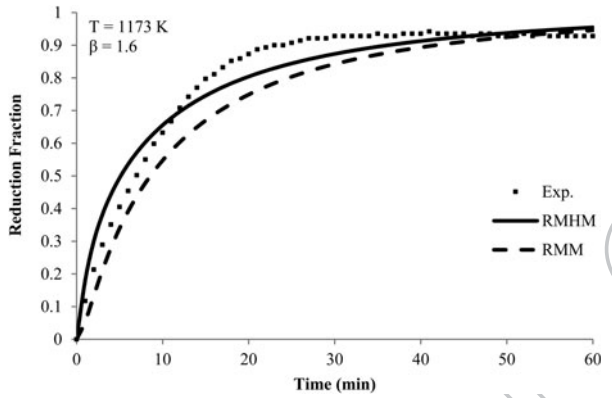

7 Comparison of the reduction fraction of the fixed bed as a function of time at 1173 K and various β, i.e. H_2/CO, between experiment results (Exp.) and two different model predictions, i.e. the RMM and the RMHM

Table 7 The difference between the actual temperature in the bed and the model output from the RMHM for various ratios of H_2/CO, i.e. (β)

β	0.8	1.2	1.6	2
Maximum ΔT	−15	−3	−9	−2

gives an error that average is more than twice as high, i.e. 2.5%. Based on this, it was concluded that the RMHM reproduced the experimental results with much less error compared to the RMM at the intermediate range of reduction fraction as shown in Fig. 7. The RMHM was therefore used to calculate the temperature drop in the bed. It should however, be mentioned that the RMHM predictions of the temperature drop in the bed were less than those actually observed and the time required to achieve thermal equilibrium proved to be over predicted. Hence the RMHM could benefit from further parameter tuning as shown in Table 7. It should also be mentioned that the constant wall temperature assumed in the model was not sufficiently valid, as the furnace controller constantly increased the power to compensate for the impact of the endothermic reactions. This resulted in a rapid temperature rise and a characteristic proportional-integral 'overshoot' in the set point as observed in Fig. 8. Hence, the temperature deviations were experimentally induced, and they were not a result of the fundamental model parameters used.

The results obtained from the experiments using pure H_2 or pure CO has also been compared to the modelling results, see Figs. 9–12. As can be seen from Fig. 9 and Fig. 11, the RMM over predicts the reduction, while the RMHM under predicts the reduction when it exceeds 50%. Error analysis was performed using equation (13), and indicative errors of 0.83% and 2.6% for the RMHM and RMM were obtained respectively.

As can be seen from Fig. 10, the deviation between the RMHM and the experimental results for reduction by H_2 is still considerable. The RMHM predictions are, however, noticeably improved when compared to the RMM with the error analysis indicting a 4.8% and 14.4% error for the RMHM and RMM respectively. The continued deviation by the RMHM may partly be explained by the power increase induced by the furnace temperature controller as mentioned previously. In the temperature profile presented in Fig. 12, this is evident as a rapid increase in temperature is obtained after the minimum has been experienced. In a comparison between Figs. 10 and 12, it is clear that the RMHM correctly accounts for the relative direction and magnitude of the 'peak' temperature deviation (positive in the case of CO due to exothermic reduction reactions, and negative for H_2 due to the endothermic reduction reactions).

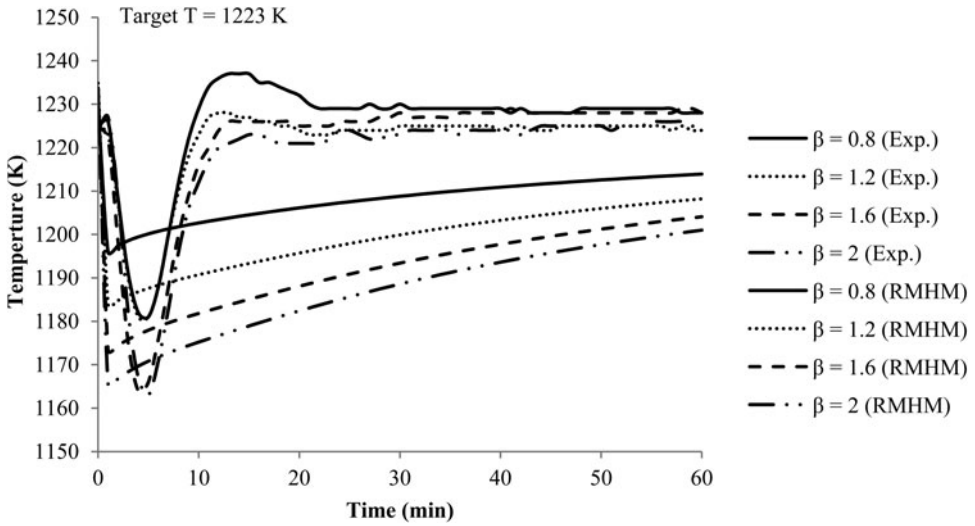

8 Comparison of the fixed bed temperature as a function of time at 1223 K and various β, i.e. H_2/CO, between the experiment results (Exp.) and the model prediction, i.e. the RMHM

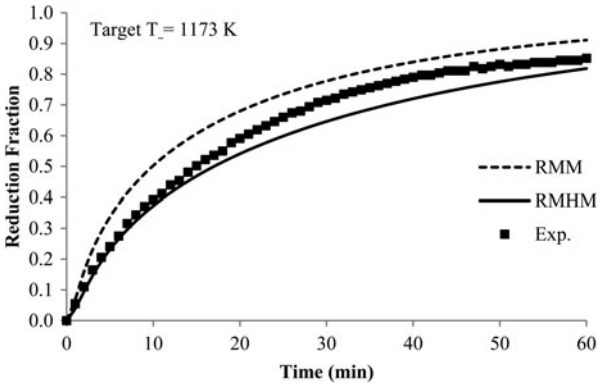

9 Comparison of the reduction fraction of the fixed bed as a function of time, at the aim temperature 1173 K in pure CO, between the experiment results (Exp.) and two different model predictions, i.e. the RMM and the RMHM

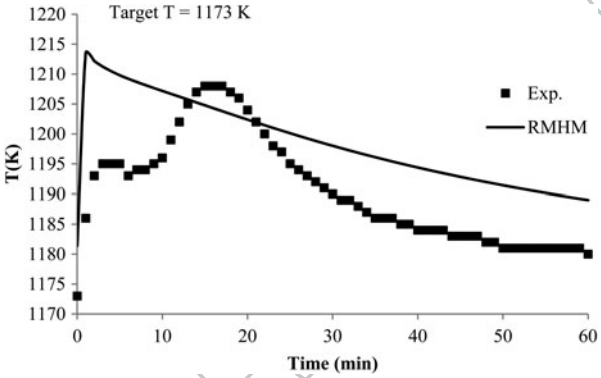

10 Comparison of the fixed bed temperature as a function of time at the aim temperature 1173 K in pure CO between the experiment results (Exp.) and the model prediction, i.e. the RMHM

In Fig. 13 the relative error between the experimental results and the RMHM predictions for $\beta = 0.8$ and $\beta = 1.6$ in the temperature interval 1123–1273 K is presented. As can be seen from the figure, in the temperature interval 1123–1223 K the RMHM reproduced the experimental results with accuracy independent of the gas composition, i.e. with an error of 1.2%. At 1273 K, the error is, however,

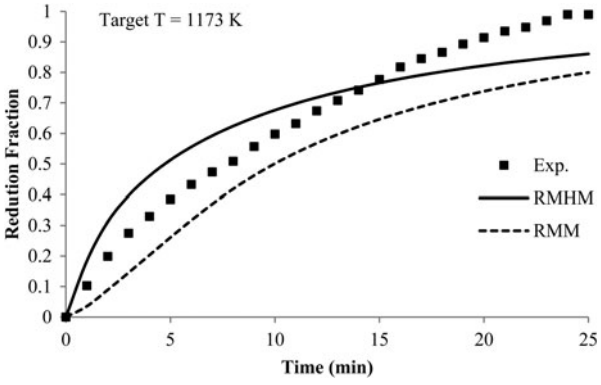

11 Comparison of the reduction fraction of the fixed bed as a function of time at the aim temperature 1173 K in pure H_2 between the experiment results (Exp.) and two different model predictions, i.e. the RMM and the RMHM

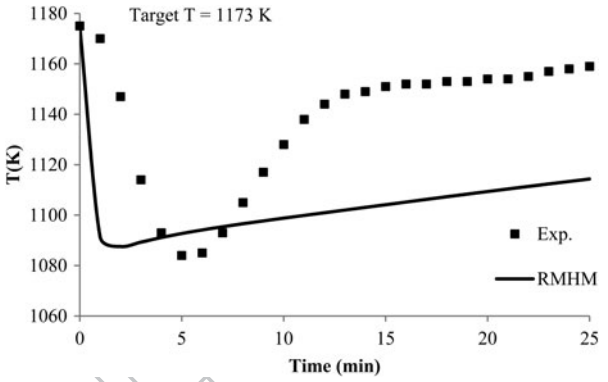

12 Comparison of the fixed bed temperature as a function of time, at aim temperature 1173 K in pure H_2 between the experiment results (Exp.) and the model prediction, i.e. the RMHM

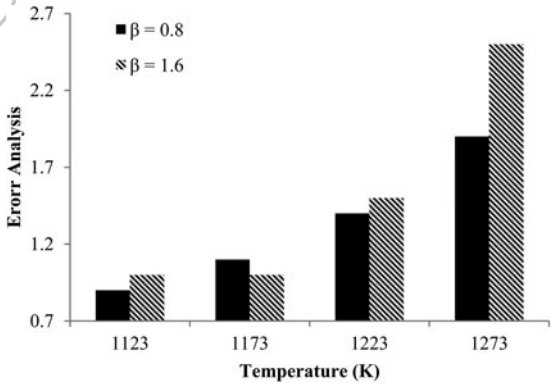

13 The error analysis for the RMHM based on equation (13) for two different gas ratios of H_2/CO (β), i.e. $\beta = 0.8$ and $\beta = 1.6$, and the temperatures 1123, 1173, 1223 and 1273 K

Table 8 The error analysis obtained for the RMHM at 1173 K and 1223 K using different gas ratios of H_2/CO, i.e. β

B	**0.8**	**1.2**	**1.6**	**2**
T (K)				
1173	1.1	1.1	1.1	1.1
1223	1.4	1.3	1.5	1.1

more significant, i.e. 2.2%, but still within an acceptable range.

The results from the calculation of individual errors obtained for the RMHM at 1173 K and 1223 K are compared in Table 8 for different gas ratios, i.e. $\beta = 0.8$–2. Although the error proved to increase at higher temperatures, the deviation was calculated to be only 1.3% at 1223 K.

Summary and conclusions

A kinetic model has been developed that describes the chemical reactions and the mass equations for each gaseous species within the bed. Since all the sequential iron oxide reduction reactions are either endothermic or mildly exothermic, it has been of interest to investigate the possibility that the model could be improved. Simultaneously considering heat transfer with the reaction

kinetics, but without unnecessarily increasing the complexity of the model and/or the computational time was the chosen strategy. Results from both models, i.e. with and without considering heat transfer, have been compared in the present study. The following major conclusions are made:

- Experimentally it was seen that the pellets were reduced quickly, i.e.70% reduction was achieved during the first 10 minutes. The overall reduction reaction was highly endothermic and caused a significant temperature drop (maximum 60 K) even in small scale beds.
- Endothermic reactions reduced the gas temperature and inhibited the reduction rate. To achieve a high rate of reaction it was necessary to either increase the temperature of the reducing gas, or to increase the level of H_2/CO ratio. At a sufficiently high temperature it is believed that the desired conversion may be achieved in a rapid manner even when a low H_2/CO ratio is used.
- Although both models, i.e. the RMM and RMHM, predict the variations observed in the experimental information, it was the more rigorous RMHM that gave the best representation of the behaviour of the reducing bed. The average error analysis for reduction at 1173 K with $\beta = 0.8–2$ proved to decrease from 2.5% in the case of the RMM to 1.1% in the case of the RMHM.
- There are some discrepancies between the experimental results and the RMHM results in the case of reduction by pure H_2 or pure CO, which were thought to be due to limitations in the experimental set-up (furnace temperature controllers) rather than fundamental issues in the model.
- The RMHM can model the presently obtained experimental results with acceptable accuracy at all gas ratios. The magnitude of the error for reduction by a gas mixture of $\beta = 1.6$ increased from 1.1% at 1173 K to 1.5% at 1223 K.
- At constant temperature, i.e. 1173 K, a typical error of 1.1% was obtained in the case of the RMHM, and a typical error of 2.5% in the case of the RMM, representing a 50% reduction in the error.

Acknowledgements

The authors would like to thank the CK-lab of LKAB in Malmberget, Sweden, for the use of the TGA (Thermal Gravity Analysis) furnace. The supply of KPRS pellets from LKAB in Kiruna, Sweden, is gratefully acknowledged. The present study was supported by BP and Nordland fylkeskommune in Norway, and LKAB in Sweden.

References

1. R. Yin: 'Considerations on steel manufacturing process', *ISIJ Int.*, 2002, **42**, (10), 1061–1064.
2. M. Gojic: 'Current state and development of steelmaking processes', *Metalurgija*, 2004, **3**, (43), 163–168.
3. T. P. Battle: 'Sustainability in ironmaking: the rise of direct reduction', in '*Proceedings of the extraction and processing division symposium on pyrometallurgy in honor of David G.C. Robertson*', (ed. P. J. Mackey *et al.*), 275–288; 2014, Hoboken, NJ, John Wiley & Sons, Inc.
4. H. K. Pinegar, M. S. Moats and H. Y. Sohn: 'Flowsheet development, process simulation and economic feasibility analysis for novel suspension ironmaking technology based on natural gas: Part 1 – flowsheet and simulation for ironmaking with reformerless natural gas', *Ironmaking Steelmaking*, 2012, **39**, (6), 398–408.
5. C. Wang, M. Larsson, C. Ryman, C. E. Grip, J. O. Wikström, A. Johnsson and J. Engdahl: 'A model on CO_2 emission reduction in integrated steelmaking by optimization methods', *Int. J. Energ. Res.*, 2008, **32**, (12), 1092–1106.
6. S. K. Dutta, A. B. Lele and N. K. Pancholi: 'Studies on direct reduced iron melting in induction furnace', *Trans. Indian Inst. Met.*, 2004, **57**, (5), 467–473.
7. A. Sawada and T. Mitamoto: 'Overview of market for direct reduced iron', *Kobelco Technol. Rev.*, 2010, **29**, 47–49.
8. B. Anameric and S. K. Kawatra: 'Properties and features of direct reduced iron', *Miner. Process. Extr. Metall. Rev.*, 2007, **28**, 59–116.
9. A. Elliot and J. Kopfle: '*New developments in the MIDREX® direct reduction process*'; 2008, Charlotte, NC, Midrex Technologies.
10. A. Chatterjee: '*Sponge iron production by direct reduction of iron oxide*'; 2012, India, PHI Learning Private Limited.
11. A. Markotic, N. Dolic and V. Trujic: 'State of the direct reduction and reduction smelting processes', *J. Min. Metall.*, 2002, **8**, (3–4), 123–141.
12. T. Battle, U. Srivastava, J. Kopfle, R. Hunter and J. McClelland: 'Chapter 1.2 — the direct reduction of iron' in '*Treatise on process metallurgy*', (ed. S. Seetharaman), 89–176; 2014, Boston, Elsevier.
13. M, R&D: '*World Direct Reduction statistics*'; 2013, Charlotte, NC, Midrex Technologies.
14. X. Jiang, L. Wang and F. M. Shen: 'Shaft furnace direct reduction technology — midrex and energiron', *Adv. Mater. Res.*, 2013, **805–806**, 654–659.
15. M. Barati: 'Energy intensity and greenhouse gases footprint of metallurgical processes: a continuous steelmaking case study', *Energy*, 2010, **35**, 3731–3737.
16. J. Aguilar, R. Fuentes and R. Viramontes: 'Simulation of iron ore reduction in a fixed bed', *Modell. Simul. Mater. Sci. Eng.*, 1995, **3**, (2), 131.
17. J. Yagi, R. Takahashi and Y. Omori: 'Study on the reduction process of iron oxide pellets in isothermal fixed bed', *Sci. Rep. Res. Inst., Tohoku University. Ser. A, Phys., Chem. Metall.*, 1971, **23**, 31–47.
18. R. Longbottom and L. Kolbeinsen: 'Iron ore reduction with CO and H2 gas mixtures — thermodynamic and kinetic modelling', 4th ULCOS Seminar, 1–2 October 2008, Essen, Germany, 1–13.
19. R. Beheshti, J. Moosberg-Bustnes and R. E. Aune: 'Modeling and simulation of isothermal reduction of a single hematite pellet in gas mixtures of H2 and CO' in '*TMS 2014 supplemental proceedings*', 495–502; 2014, Hoboken, NJ, John Wiley & Sons, Inc.
20. O. Levenspiel: '*Chemical reaction engineering*', 1999, Hoboken, NJ, USA, John Wiley & Sons.
21. J.-I. Yagi and J. Szekely: 'The effect of gas and solids maldistribution on the performance of moving-bed reactors: the reduction of iron oxide pellets with hydrogen', *AIChE J.*, 1979, **25**, (5), 800–810.
22. L. Kolbeinsen: 'Modelling of DRI processes with two simultaneously active reducing gases', *Steel Res. Int.*, 2010, **81**, (10), 819–828.
23. J. Szekely, J. W. Evans and H. Y. Sohn: '*Gas-solid reaction*'; 1976, New York, USA, Academic Press.
24. M. S. Valipour: 'Mathematical modeling of a non-catalytic gas-solid reaction: hematite pellet reduction with syngas', *Trans. C: Chem. Chem. Eng.*, 2009, **16**, (2), 108–124.
25. R. Beheshti, J. Moosberg-Bustnes, M. William Kennedy and R. E. Aune: 'Reduction of commercial hematite pellet in isothermal fixed bed—experiments and numerical modelling', *Ironmaking Steelmaking*, 2015.
26. J. Shi, E. Donskoi, D. L. S. McElwain and L. J. Wibberley: 'Modelling the reduction of an iron ore-coal composite pellet with conduction and convection in an axisymmetric temperature field', *Math. Comput. Modell.*, 2005, **42**, (1–2), 45–60.
27. M. S. Valipour and Y. Saboohi: 'Modeling of multiple noncatalytic gas–solid reactions in a moving bed of porous pellets based on finite volume method', *Heat Mass Transfer*, 2007, **43**, (9), 881–894.
28. A. Rahimi and A. Niksiar: 'A general model for moving-bed reactors with multiple chemical reactions part I: model formulation', *Int. J. Min. Process.*, 2013, **124** (November), 58–66.
29. S. Sun and W. K. Lu: 'Mathematical modelling of reactions in iron ore/coal composites', *ISIJ Int.*, 1993, **33**, (10), 1062–1069.
30. FactSage: 'Reaction-Web', 2015 [viewed 2015 23.08.2015]; Available from: http://www.crct.polymtl.ca/reacweb.htm.
31. F. Patisson and D. Ablitzer: 'Modeling of gas-solid reactions: kinetics, mass and heat transfer, and evolution of the pore structure', *Chem. Eng. Technol.*, 2000, **23**, (1), 75–79.
32. LKAB: '*LKAB product booklet*'; 2013, Sweden, LKAB.
33. R. Beheshti, J. Moosberg-Bustnes, M. W. Kennedy and R. E. Aune: 'Reduction of commercial hematite pellet in an isothermal fixed bed

— experiments and numerical modelling', *Ironmaking Steelmaking*, 2015.
34. Y. Takenaka, Y. Kimura, K. Narita and D. Kaneko: 'Mathematical model of direct reduction shaft furnace and its application to actual operations of a model plant', *Comput. Chem. Eng.*, 1986, **10**, (1), 67–75.
35. S. M. M. Nouri, H. Ale Ebrahim and E. Jamshidi: 'Simulation of direct reduction reactor by the grain model', *Chem. Eng. J.*, 2011, **166**, (2), 704–709.
36. D. R. Parisi and M. A. Laborde: 'Modeling of counter current moving bed gas-solid reactor used in direct reduction of iron ore', *Chem. Eng. J.*, 2004, **104**, 35–43.
37. N. Towhidi and J. Szekely: 'Reduction kinetics of commercial low-silica hematite pellets with CO-H_2 mixture range 600–1232°C', *Ironmaking Steelmaking*, 1981, **6**, 237–249.
38. E. T. Turkdogan and J. V. Vinters: 'Gaseous reduction of iron oxides: part I. Reduction of hematite in hydrogen', *Metall. Mater. Trans. B*, 1971, **2** (November), 3175–3188.
39. J. O. Edstrom: 'The mechanism of reduction of iron oxide', *J. Iron Steel Inst.*, 1953, **175**, 289–304.
40. A. A. Poli and M. C. Cirillo: 'On the use of the normalized mean square error in evaluating dispersion model performance', *Atmos. Environ.. Part A. Gen. Top.*, 1993, **27**, (15), 2427–2434.